Combing of genomic DNA from droplets containing picograms of material

Deen, Jochem; Sempels, Wouter; De Dier, Raf; Vermant, Jan; Dedecker, Peter; Hofkens, Johan; Neely, Robert K.

Combing of Genomic DNA from Droplets Containing Picograms of Material

Jochem Deen,[†,▽] Wouter Sempels,[†,▽] Raf De Dier,[‡] Jan Vermant,[‡,§] Peter Dedecker,[†] Johan Hofkens,[†,∥] and Robert K. Neely*[,†,⊥]

[†]Department of Chemistry, KU Leuven, Celestijnenlaan 200F, Heverlee 3001, Belgium, [‡]Department of Chemical Engineering, KU Leuven, Willem de Croylaan 46, Heverlee 3001, Belgium, [§]Department of Materials, ETH Zürich, Vladimir Prelog Weg 5, CH 8093 Zürich, Switzerland, [∥]Department of Chemistry, University of Copenhagen, Universitetsparken 5, 2100 Copenhagen, Denmark, and [⊥]School of Chemistry, University of Birmingham, Edgbaston, Birmingham B15 2TT, United Kingdom. [▽]These authors (J.D. and W.S.) contributed equally

ABSTRACT Deposition of linear DNA molecules is a critical step in many single-molecule genomic approaches including DNA mapping, fiber-FISH, and several emerging sequencing technologies. In the ideal situation, the DNA that is deposited for these experiments is absolutely linear and uniformly stretched, thereby enabling accurate distance measurements. However, this is rarely the case, and furthermore, current approaches for the capture and linearization of DNA on a surface tend to require complex surface preparation and large amounts of starting material to achieve genomic-scale mapping. This makes them technically demanding and prevents their application in emerging fields of genomics, such as single-cell based analyses. Here we describe a simple and extremely efficient approach to the deposition and linearization of genomic DNA molecules. We employ droplets containing as little as tens of picograms of material and simply drag them, using a pipet tip, over a polymer-coated coverslip. In this report we highlight one particular polymer, Zeonex, which is remarkably efficient at capturing DNA. We characterize the method of DNA capture on the Zeonex surface and find that the use of droplets greatly facilitates the efficient deposition of DNA. This is the result of a circulating flow in the droplet that maintains a high DNA concentration at the interface of the surface/solution. Overall, our approach provides an accessible route to the study of genomic structural variation from samples containing no more than a handful of cells.
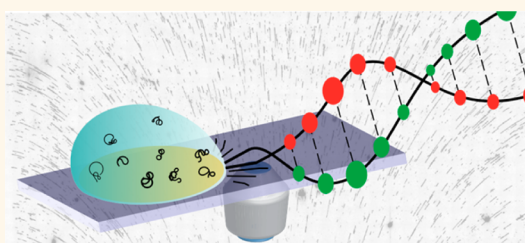
KEYWORDS: molecular combing · DNA mapping · fiber-FISH · DNA deposition · rolling droplet · coffee ring effect · single-molecule imaging

DNA mapping[1−4] and fiber-FISH[5,6] experiments are routinely used in the study of genome structure[7−11] and the physical validation of sequence assemblies[12−15] as well as in diagnostic[16−19] and epigenomic studies.[20−23] Crucially, these experiments offer a tool that is rapid to implement and derives information on a large scale, which complements that typically derived from sequencing. Emerging sequencing technologies, such as those employing electron microscopy,[24] promise to link this long-range information with a base-by-base readout.

With the exception of nanochannel-based approaches, which are technically extremely demanding, all of these technologies rely on the deposition and linearization of DNA on a surface for imaging. In an ideal case, the DNA that is deposited is absolutely linear and uniformly stretched

such that accurate distance measurements (with units of (kilo)base pairs) can be made along the DNA molecule. Furthermore, for emerging applications, such as single-cell mapping[11,25] where the concentration of DNA is as low as picograms per microliter, the efficiency of the DNA deposition process must be extremely high.

There are two important elements that enable the deposition of linearized DNA molecules, i.e., a surface capable of spontaneous DNA capture and a mechanism to extend the DNA. Typically, DNA is deposited using either a surface carrying a net positive charge (e.g., functionalized with poly-L-lysine) that attracts the negatively charged DNA backbone or a surface modified with a hydrophobic compound.[26]

In the first case, deposition of DNA on a positively charged surface requires an

©2015 American Chemical Society

extensional force from a flowing solution in order to linearize the DNA.[27] This force arises as a result of a velocity gradient close to the surface, along the direction of flow.[28] Several methodologies have been proposed to create this flow, most notably microfluidic chambers,[29] spin-coating,[30,31] capillary flow in evaporating droplets,[32,33] or simply smearing a solution across a surface by dropping a glass slide onto a droplet.[34,35] While DNA deposition efficiency is high using this approach, the DNA is prone to large deviations in direction during deposition, and this can make it difficult to reliably measure distances along the DNA molecule.

In the second case, the deposition of DNA on a hydrophobic surface, a pH of approximately 6 encourages partial melting of the duplex and facilitates spontaneous tethering of the DNA at its extremities to the surface.[36] This approach, known as molecular combing,[37] relies on translation of the liquid–air interface (commonly referred to as the meniscus) over the tethered DNA, uniformly overstretching the DNA to 150% of its crystallographic length.[26] The stretching of molecules is independent of fluid flow and instead is dependent upon the surface tension at the receding contact line.[26] DNA molecules deposited in this way are aligned perpendicular to the moving contact line, improving the reproducibility of measurements along the molecule.

The most notable attempts for creating a moving contact line have been by the use of a reservoir into which the modified coverslip is dipped[5,36,38] and using an evaporating droplet on the modified coverslip.[37,39] While these approaches work well for many applications, they suffer from several practical drawbacks. For example, the use of a reservoir of DNA solution into which a coverslip is immersed and then slowly withdrawn requires a relatively large amount of starting material (e.g., Michalet et al.[5] use a total of 1 mg DNA in a 4 mL reservoir), while an evaporating droplet is severely limited in the surface area it can cover (ca. 0.73 mm^2 for a droplet of 2 μL on a hydrophobic surface) and hence the amount of material that can be deposited.

The hydrophobic surfaces for molecular combing are generally functionalized using silane chemistry.[5,26,36,37,40−42] However, numerous reports in the literature have shown that the structure and quality of this silane film are critically dependent on the dryness of the solution, humidity, temperature, reaction time, and pretreatment of the substrate.[38,43−47] In our experience, these parameters can prove rather difficult to control under standard laboratory conditions. As an alternative, some groups have attempted to use polymer spin-coating as opposed to silanization. Most notable among the polymers employed for this purpose are poly(methyl methacrylate) (PMMA),[36,39,41] polydimethylsiloxane (PDMS),[40] and polystyrene (PS).[36]

We experimented with many of these approaches for DNA deposition and were surprised to find one polymer, Zeonex, which has remarkable performance in terms of DNA capture, in comparison to the others we tested. We focused on using this polymer to develop a reproducible, robust method for DNA deposition. Our goal has been to understand and optimize deposition efficiency with the aim of producing a uniform surface coverage of DNA molecules that are stretched in a predictable fashion, from small sample volumes and at low DNA concentrations (i.e., picograms per microliter).

RESULTS AND DISCUSSION

Here, we compare three different hydrophobic substrates for DNA combing. These polymers have distinct chemical properties in terms of their ability to form hydrogen bonds and their polarizability. PMMA is the least hydrophobic of the tested substrates, with some propensity for hydrogen bond formation and has been employed for DNA combing previously.[36,39,41] Zeonex is a cyclic olefin polymer that is polarizable but which has negligible hydrogen-bonding character, and CYTOP is a fluorinated polymer with low polarizability and essentially no hydrogen-bonding character. All substrates are stable under ambient conditions and compatible with studies at the single-molecule level using a fluorescence microscope (i.e., they are optically transparent and contain little or no fluorescent impurities). The polymers are readily deposited onto a glass microscope slide using spin-coating. We initially examined the affinity of each surface for DNA by using an evaporating droplet for deposition and combing. By far the most efficient DNA deposition is observed on the Zeonex surface, followed by PMMA and CYTOP, where barely any DNA is deposited at all (Supporting Information, Figure 1).

We observed two distinct phases during evaporation of droplets with DNA (Supporting Information, Figure 2) on Zeonex and CYTOP. The first phase shows evaporation of the droplet and a decrease of the contact angle while the droplet is pinned at the same location. During this phase DNA molecules will accumulate at the contact line due to the well-known coffee ring effect.[43] During the second phase, the contact angle remains mostly constant while the width of the droplet decreases, and DNA molecules are deposited linearly on the surface. Consistent with previous reports,[48] on the PMMA a more complex behavior is seen and a partial mixing of these modes and phases occurs.

Deposition of DNA on the PMMA is critically dependent on the accumulation of DNA at the droplet edge, which predominantly occurs during the early phases of the droplet evaporation. By comparison, relatively little DNA is tethered to the surface during the latter phases of evaporation. Hence, the coffee ring effect
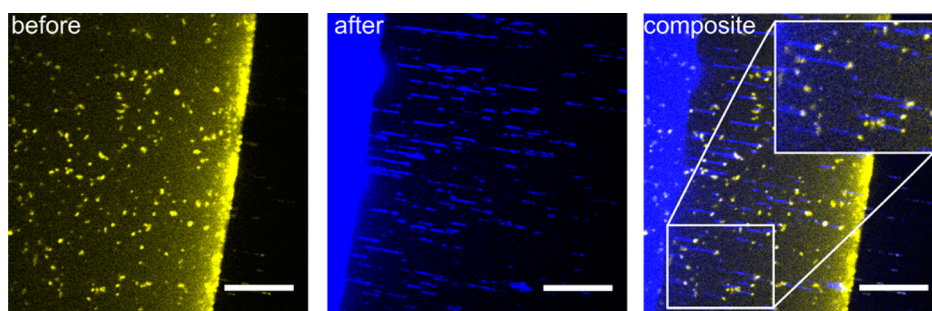
Figure 1. DNA deposition on Zeonex from an evaporating droplet. DNA forms a stable attachment to the surface (yellow image), and the vast majority of these molecules are stretched (blue) as the contact line moves over them as shown in the merged image. DNA molecules are stained with 50 nM SYBR Gold. Scale bar is 20 μm in length.
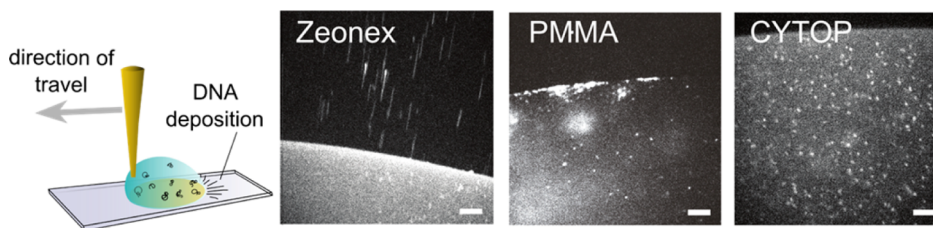

Figure 2. Schematic representation of our rolling droplet experiment and microscope images taken of DNA deposition at the edge of droplets translated across the three different surfaces. Deposition is far more efficient on the Zeonex surface than other substrates. The surface is translated below the droplet with a speed of 1.5 mm/min. Scale bars are 10 μm in length. DNA is stained with 50 nM SYBR Gold dye (a nonspecific, groove-binding fluorophore).

and the accumulation of a high DNA concentration at the solution–air–surface interface play a critical role in the DNA deposition process on PMMA. In the case of Zeonex, however, DNA molecules are tethered to the surface over the entire droplet–surface interface continuously and throughout the evaporation process, as shown in Figure 1. As the contact line moves over these molecules, the majority (approximately 60%) are stretched, with the remainder detaching from the surface. Our results indicate that the Zeonex surface forms a far stronger interaction with the DNA than does the PMMA. This efficient end-tethering of DNA on a surface that is both hydrophobic and polarizable is consistent with the model of partial DNA melting at the extremities and the association of the bases with the surface, previously observed during molecular combing experiments. The potential ability of the surface to form hydrogen-bonding interactions with the DNA plays a far less significant role in the DNA tethering process, under the conditions we employ.

Deposition using an evaporating droplet is neither an efficient nor predictable means for achieving the deposition of large genomes. To achieve a uniform DNA deposition density across square millimeters of substrate, we developed a system to translate a microliter droplet of solution slowly across a surface, shown schematically in Figure 2. Our approach simply involves lowering a disposable pipet tip until it contacts the droplet. Once the droplet is anchored on the pipet tip (using capillary forces), the tip is used to drag the droplet slowly across the surface. Tip motion is controlled using a stepper motor. In this way, the droplet

can be translated across several centimeters of surface with a constant velocity. This approach exploits the ability, that we observed in the evaporating droplets, of the Zeonex polymer to spontaneously capture DNA from solution. Images taken at the edge of the droplet during translation, for each of the surfaces, are shown in Figure 2 (and in Supporting Information, Videos 1–3). We routinely deposited DNA across tens of square millimeters using this approach.

We determined the DNA deposition efficiency on each of the three surfaces by measuring its concentration (using SYBR Gold as a DNA stain) before and after droplet translation across 5 cm of surface at a constant velocity of 4 mm/min. We found, using an initial concentration of 100 pg/μL of DNA and a 2 μL droplet, that 96% ($\pm$7%) of starting material remained in the droplet after it was translated across the CYTOP surface, compared with 90% ($\pm$8%) of the starting material in the droplet on PMMA and only 74% ($\pm$11%) of the starting material in the droplet on the Zeonex (Supporting Information, Figure 3). To put this into some context, a deposition efficiency of 25% and a starting concentration of just 100 pg/μL of DNA would result in the deposition of approximately 480 kilobase pairs of DNA (corresponding to 12 bacteriophage T7 molecules) per CCD image (55 $\times$ 55 μm). At this deposition density, optical mapping of the *E. coli* genome to 100$\times$ depth ($\sim$500 megabases) would require around 210 images in total; around 3–4 min of imaging time. Measurement of the length of deposited phage lambda genomic DNA molecules on Zeonex gives a mean length of 27.6 μm with a
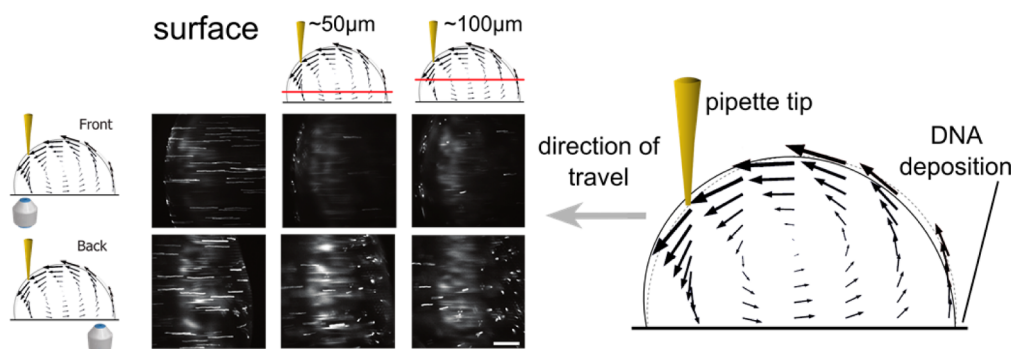
Figure 3. Long-exposure confocal microscopy images using fluorescent tracer beads to depict the flow in a microliter droplet as it is translated across a Zeonex-coated substrate. The six microscopy images show the movement of the tracer beads at the front (close to the pipet tip) and the back of the droplet, at different depths for a 5 s camera exposure. Note that there are approximately five times more particles at the surface interface compared with the bulk solution. Scale bar is 100 μm. The right panel shows the modeled flow profile in the droplet, in the reference frame of the droplet, derived using the microscopy data. Arrows are vectors indicating the velocity of the flow around the droplet. The circulating flow in the droplet results in a continuous supply of DNA molecules to the surface, where they can subsequently bind the surface and be stretched.

standard deviation of 1.2 μm; a stretching factor of 1.67 times the solution-phase contour length (16.5 μm) of this DNA molecule (Supporting Information, Figure 4).

Aqueous droplets translating across hydrophobic surfaces tend to move using two distinct mechanisms, *i.e.*, slipping and rolling.[49,50] In order to better understand the mechanisms contributing to DNA deposition in our translating droplets we developed a setup allowing us to image the flow within the droplet as it was moved across the Zeonex-coated surface. We maintained the droplet above our objective using a pipet tip and slowly translated the substrate below the droplet. Fluorescent tracer beads in the droplet combined with long exposures (5 s) of the camera show that rather than a capillary flow toward the edge of the droplet (as observed in evaporating droplets), we see a caterpillar track-like flow in the translating droplet, Figure 3, which is clearly rolling across the Zeonex. The flow has the effect of maintaining a constant concentration of the tracer beads at the surface of the substrate, and we see the same behavior with DNA molecules. Flow is driven by the relatively rapidly moving substrate and slows toward the center of the droplet. We used this observed flow profile, particularly in the region close to the translating surface, in order to inform a more complete model of the flow in the droplet. Based on the previously reported model of Mognetti *et al.*,[49] the resulting velocity profile, given for a vertical cross-section of the rolling droplet parallel to the direction of the droplet travel, is shown in Figure 3. Crucially, in the rolling droplet we observe 4−5 times more tracer particles at the solid−liquid interface compared to the bulk of the solution (Supporting Information, Figure 5).

We examined the effect of slowing the translation speed of the droplet on the DNA deposition efficiency on Zeonex. The model of rolling flow in the droplet indicates that slowing translation would both increase the duration that DNA molecules spend in close

proximity to the surface (increasing the likelihood of tethering) and decrease the speed of the upward flow at the trailing edge of the droplet (decreasing the likelihood of detachment of DNA molecules from the surface). Indeed, we found a significant increase in deposition efficiency with decreasing translation speed from 2.1 gigabase pairs per mm^2 at 2 mm/min to 0.5 gigabase pairs per mm^2 at a translation speed of 8 mm/min (based on deposition of 40 kilobase pair T7 phage genomic DNA molecules, Supporting Information, Figure 3).

In order to demonstrate the efficient deposition of large DNA molecules, we deposited human genomic DNA and created a composite image of the stretched molecules on a Zeonex surface. We diluted the DNA sample to just 170 and 40 pg in two 1 μL droplets, equivalent to the DNA content of approximately 26 and 6 human cells per droplet, respectively. We observed efficient deposition of DNA molecules of up to 300 kilobase pairs in length from these droplets, as shown in Figure 4, though the vast majority of the DNA molecules are fragmented (due to handling prior to deposition) to lengths between 15 and 80 kbp (Supporting Information, Figure 6). While it was possible to deposit far longer DNA molecules (Supporting Information, Figure 7), protection of DNA against shearing prior to deposition was challenging. Furthermore, because of the continuous, circulating flow within the droplet, the deposition efficiency is uniform across the region over which the droplet has been translated.

Finally, in order to demonstrate the applicability of DNA deposition on Zeonex to optical DNA mapping, we extracted bacterial (*E. coli* strain ER2566) genomic DNA, labeled this at specific sites (5′-TCGA-3′) using the two-step methyltransferase-directed (commercially available M.*Taq*I DNA methyltransferase) click chemistry we reported previously.[51] Figure 5 shows the resulting densely deposited DNA from a 1 μL droplet containing 1 ng of bacterial genomic DNA.
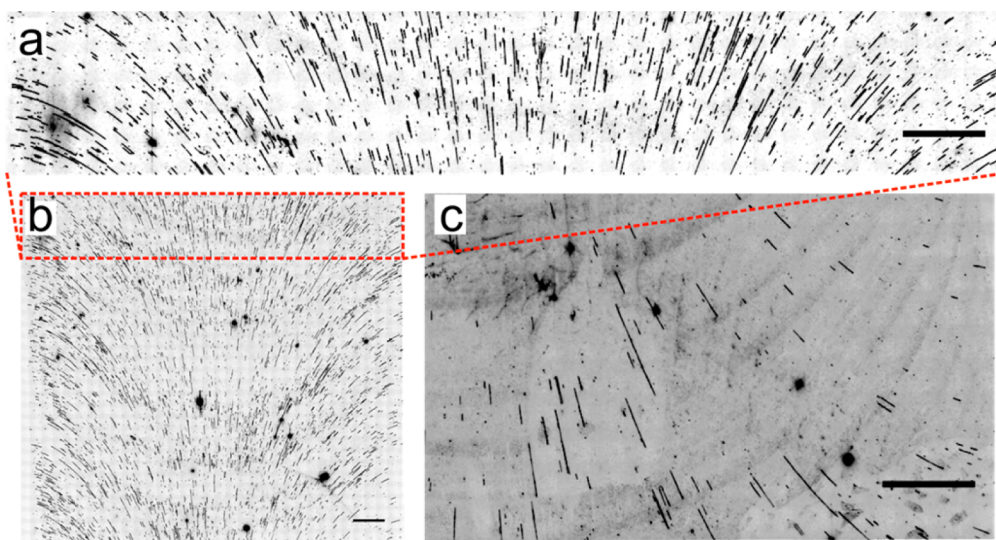
Figure 4. Fluorescence microscopy images (using an inverted look-up table, where black depicts high photon counts) of YOYO-1-stained human genomic DNA (extracted from HeLa cells) deposited from a 1 μL droplet containing (a, b) approximately 170 pg of DNA or (c) 40 pg of DNA. All scale bars are 200 kilobase pairs in length (108 μm). DNA is deposited and linearized perpendicular to the edge of the rolling droplet resulting in a characteristic deposition pattern.
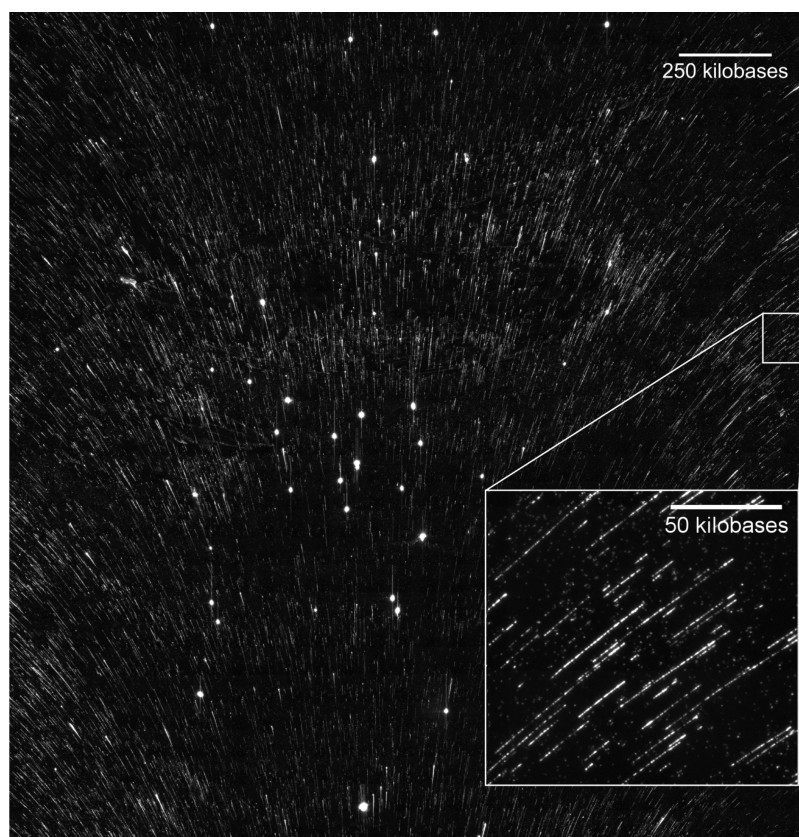

Figure 5. A total of 1225 tiled fluorescence microscopy images of a sample of E. coli genomic DNA labeled with Atto647N at sites reading 5′-TCGA-3′ using the M.*Taq*I DNA methyltransferase enzyme in order to direct labeling. The image contains approximately 500 megabases of genomic material and took of the order of 10 min to acquire.

CONCLUSION

We have identified a simple, reproducible procedure for the deposition of DNA on Zeonex-coated microscope slides. The Zeonex polymer has proven remarkably efficient at trapping DNA molecules, compared with the other substrates (PMMA and CYTOP) we tested. We measured an average 26% deposition efficiency on Zeonex when translating a droplet over 20 mm, compared to

10% for PMMA and 4% for CYTOP. This efficiency is the result of the end attachment of DNA molecules to the Zeonex surface, which happens spontaneously for DNA molecules in solution on a Zeonex surface under our experimental conditions at pH 5.7.

By translating a droplet of DNA over this surface we can achieve uniform surface coverage of DNA molecules. Our confocal measurements on the translating droplet showed an internal circulating belt-like flow, consistent with rolling of the droplet across the surface. The circulating flow results in a high concentration of DNA molecules at the interface with the surface, and we are able to exploit this, along with the ability of Zeonex to spontaneously adsorb DNA from solution in order to control the DNA deposition efficiency. Translation of a droplet containing around a hundred picograms of DNA across the Zeonex surface enables efficient deposition of gigabases of megabase pair-long DNA molecules. By simply reducing droplet translation velocity, DNA can be deposited from droplets containing minute amounts of material (a few picograms) for subsequent single-molecule, single-cell genomic analyses. The key to progressing this approach to single-cell applications will lie in our ability to extract and purify DNA from single cells and to subsequently isolate this DNA in droplets. Single-cell DNA isolation and manipulation[52] are already being applied in genomics, and as a result the capture of all of the genomic material from a single cell on a surface in the near future is a real possibility.

METHODS

All materials were purchased from Sigma-Aldrich and used as described by the manufacturer, unless stated otherwise

Preparation of Glass Substrates. Glass coverslips (22 × 22 mm, Menzel-Gläser no. 1.5, Germany) were cleaned to remove any fluorescent contaminants by incubation in a furnace oven at 450 °C for 24 h prior to functionalization.

Zeonex (Zeon Chemicals L.P.) was prepared as a 1.5% w/v solution in chlorobenzene poly(methyl methacrylate) (PMMA) was prepared as a 1.5% w/v solution in chloroform and CYTOP (CYTOP CTL-809M, Bellex International Corporation) as a 3% w/w in the solvent supplied by the manufacturer. A few drops of each solution were deposited onto a stationary coverslip and were subsequently spun at 3000 rpm for 90s. The coated coverslips were subsequently dried at 110 °C for at least 1 h, prior to use. The coated coverslips can be stored in a desiccator for several weeks without any noticeable change in their ability to bind DNA.

DNA Extraction and Staining. A solution containing either *E. coli* (ER2566) or HeLa cells was mixed in a 1:1 ratio with molten 1.5% low melting point agarose and allowed to cool. Cells were lysed by soaking the cooled agarose plugs overnight in a solution containing 50 mM ethylenediaminetetraacetic acid, 0.1% w/v sodium dodecyl sulfate, and 0.2 mg/mL proteinase K. Following lysis the plugs were washed two times in 50 mL of water for 1 h. For staining with YOYO-1, approximately 50 μg of the cleaned agarose was mixed with 50 μL of buffer containing 20 mM PIPES (pH 6.8) and 100 mM NaCl. The agarose was melted by heating to 72 °C for 15 min, cooled to 42 °C, and then digested by addition of 2 μL β-agarase (Fermentas) with incubation for 2 h at 42 °C. DNA concentration was determined by UV absorption at 260 nm, the sample was diluted in MES buffer (pH 5.7) containing 200 nM YOYO-1. This solution was incubated at 55 °C for 20 min prior to deposition. All pipetting was done using a wide-bore pipet tip to minimize unwanted shearing of the DNA.

Bacteriophage T7 DNA and bacteriophage lambda DNA (Yorkshire Bioscience) were diluted to a concentration of 100 pg/μL in 50 mM MES buffer (pH 5.7) containing 50 nM SYBR Gold or 200 nM YOYO-1 (Life technologies) and treated in the same way as the human genomic DNA.

Methyltransferase-Directed DNA Labeling. A washed agarose plug (approximately 70 μg) containing *E. coli* genomic DNA was heated to 72 °C, then cooled to 60 °C, and held at this temperature on a dry heat block. To the molten agarose we added 10 μL of NEB cutsmart buffer, 10 μL of M.TaqI DNA methyltransferase (New England Biolabs) and 10 μL of 1 mM AdoEnYn cofactor (5′-[(S)-[(3S)-3-amino-3-carboxylpropyl](E)-pent-2-en-4-ynylsulfonio]-5′-deoxyadenosine).[51] This mixture was incubated at 60 °C for 2 h and subsequently cooled to 50 °C when 2.5 μL of 20 mg/mL proteinase K was added. This was allowed to incubate for a 1 h and then cooled to

allow the agarose to solidify. Fluorescent DNA labeling was carried out by melting approximately 80 μg of agarose plug containing the M.TaqI-modified DNA and adding to this 1 μL of 20 mM Atto647N-azide [dissolved in dimethyl sulfoxide (DMSO)], 1 μL 200 μM CuSO₄, 25 μL 2 mM THPTA (tris[(1-hydroxypropyl-1H-1,2,3-triazol-4-yl)methyl]amine), and 10 μL of 50 mM sodium ascorbate. This reaction was allowed to proceed for 30 min at 40 °C after which the agarose was cooled and washed in 50 mL phosphate buffered saline solution. Finally, to remove the remaining unbound dye from the sample, the agarose was digested with β-agarase (Fermentas) incubation for 2 h at 42 °C and the DNA subject to two ethanol precipitations with resuspension in phosphate buffered saline. This purified, labeled DNA was deposited on Zeonex as described for the T7 and lambda phage genomes with the exception that no nonspecific DNA stain was added to the sample prior to deposition.

DNA Deposition. Two μL droplets of the aqueous DNA solution were deposited onto a functionalized glass coverslip, and a clean, disposable pipet tip was lowered to contact the droplet surface. The droplet is translated by moving the tip at a constant speed using a geared motor in order to ensure uniform deposition of the DNA. DNA deposition was imaged by sliding the glass substrate over the microscope objective, while holding the droplet in place using a plastic micropipette tip. For convenience, we used Eppendorf brand tips 0.1–10 μL, but no impact on the amount of deposited DNA was noted if the tip was larger or, indeed a glass capillary was employed for this purpose. DNA deposition efficiency measurements at the slowest translation speed (2 mm/min) were performed in a sealed chamber in a humid environment in order to minimize evaporation from the droplet. Again, we noted no effect of humidity on the DNA deposition efficiency. Rather, we employ the chamber (a sealed plastic box into which we stream humid air) in order to minimize droplet evaporation over the ~30 min period that we used for deposition at this very slow translation speed.

Imaging. Confocal microscopy was carried out on an adapted VTHawk system (VisiTech) using Olympus oil immersion objectives of 20× (0.85 NA) and 100× (1.4 NA). Images were recorded using an EM-CCD camera (C9100−13, Hamamatsu) with scan speeds for the full frame ranging from 0.1 to 10 Hz. Excitation of fluorophores was achieved using a 488 nm diode laser, reflected by a 405/488 nm dual band dichroic filter and a 488 nm, 10 nm band-pass excitation filter. Emission was collected *via* a 500 nm long pass emission filter.

Wide-field imaging was performed using an Olympus IX-83 microscope with a 200 mW 488 nm diode laser coupled to the microscope *via* a quad band (405/488/561/635) dichroic filter. Emission was collected *via* a quad band (25 nm band-pass 446/523/600/677) emission filter coupled to a Hamamatsu Image-EM EM-CCD camera. Sample scanning was performed using a Märzhäuser SCAN IM 120 × 80 stage. All microscope

components were synchronized/controlled using Olympus Xcellence software. Images were stitched using software written in Igor Pro (Wavemetrics).

The "tracer beads" we used were 1 μm fluorescent yellow-green beads (Life technologies). The 2% w/v stock solution was diluted 1000-fold for measurements of the flow in the droplets.

Contact Angle Measurements. Contact angle measurements were performed home-built setup using a webcam to image the droplet profile while it was mounted on the microscope. The system was compared with standard equipment and proven to give the same results. The contact angles were calculated based on software written in Matlab (Mathworks).

DNA Concentration in Droplets. DNA concentrations were determined by measuring fluorescence emission intensity of SYBR Gold using an FLS 980 spectrometer (Edinburgh Instruments). Two μL of sample was added to 98 μL water containing 50 nM SYBR Gold (100,000 times dilution of the stock solution) (Life Technologies). Fluorescence spectra were recorded using 488 nm excitation wavelength, with 5 nm wide slits for the excitation and emission paths and a 1s integration time. Fluorescence emission intensity at 550 nm was compared to emission of samples with known concentration.

Modeling of Droplet Flow Profile. A model of the flow profile in the rolling droplet was generated using Comsol Multiphysics (Comsol Inc.). The model is based on previous work by Mognetti and Thampi.[49,50]

Conflict of Interest: The authors declare no competing financial interests.

Supporting Information Available: Microscopy images of DNA deposition on three different surfaces at the beginning and end stages of droplet evaporation. Plots showing the effect of evaroration on the contact angle of droplets containing DNA on three different surfaces. Histogram of size distribution of phage lambda DNA deposited using rolling droplet method. Plot showing DNA deposition efficiency as a function of surface and droplet travel speed. Plot showing the speed of the flow in the droplet and number of molecules at each position above the surface. Microscopy image of human genomic DNA deposited from a droplet containing 200 pg of material. Microscopy movies showing deposition of DNA from a moving droplet. Histogram of size distribution of human genomic DNA deposited using the rolling droplet method. This material is available free of charge *via* the Internet at http://pubs.acs.org

REFERENCES AND NOTES

1. Neely, R. K.; Deen, J.; Hofkens, J. Optical Mapping of DNA: Single-Molecule-Based Methods for Mapping Genomes. *Biopolymers* **2011**, *95*, 298–311.

2. Samad, A. H.; Cai, W. W.; Hu, X.; Irvin, B.; Jing, J.; Reed, J.; Meng, X.; Huang, J.; Huff, E.; Porter, B.; et al. Mapping the Genome One Molecule at a Time - Optical Mapping. *Nature* **1995**, *378*, 516–517.

3. Teague, B.; Waterman, M. S.; Goldstein, S.; Potamousis, K.; Zhou, S.; Reslewic, S.; Sarkar, D.; Valouev, A.; Churas, C.; Kidd, J. M.; et al. High-Resolution Human Genome Structure by Single-Molecule Analysis. *Proc. Natl. Acad. Sci. U.S.A.* **2010**, *107*, 10848–10853.

4. Kim, S.; Gottfried, A.; Lin, R. R.; Dertinger, T.; Kim, A. S.; Chung, S.; Colyer, R. A.; Weinhold, E.; Weiss, S.; Ebenstein, Y. Enzymatically Incorporated Genomic Tags for Optical Mapping of DNA-Binding Proteins. *Angew. Chem., Int. Ed.* **2012**, *51*, 3578–3581.

5. Michalet, X.; Ekong, R.; Fougerousse, F.; Rousseaux, S.; Schurra, C.; Hornigold, N.; Slegtenhorst, M. v.; Wolfe, J.; Povey, S.; Beckmann, J. S.; et al. Dynamic Molecular Combing: Stretching the Whole Human Genome for High-Resolution Studies. *Science* **1997**, *277*, 1518–1523.

6. Weier, H.-U.; Chu, L. Quantitative DNA Fiber Mapping in Genome Research and Construction of Physical Maps. In *Gene Mapping, Discovery, and Expression*; Bina, M., Ed. Humana Press: New York, 2006; Vol. 338, pp 31–57.

7. Molina, O.; Blanco, J.; Anton, E.; Vidal, F.; Volpi, E. V. High-Resolution FISH on DNA Fibers for Low-Copy Repeats Genome Architecture Studies. *Genomics* **2012**, *100*, 380–386.

8. Pauciullo, A.; Fleck, K.; Lühken, G.; Di Berardino, D.; Erhardt, G. Dual-Color High-Resolution Fiber-FISH Analysis on Lethal White Syndrome Carriers in Sheep. *Cytogenet. Genome Res.* **2013**, *140*, 46–54.

9. Zhang, H.; Koblizkova, A.; Wang, K.; Gong, Z.; Oliveira, L.; Torres, G. A.; Wu, Y.; Zhang, W.; Novák, P.; Buell, C. R.; et al. Boom-Bust Turnovers of Megabase-Sized Centromeric DNA in Solanum Species: Rapid Evolution of DNA Sequences Associated with Centromeres. *Plant Cell* **2014**, *26*, 1436–1447.

10. Shimojima, K.; Okamoto, N.; Inazu, T.; Yamamoto, T. Tandem Configurations of Variably Duplicated Segments of 22q11.2 Confirmed by Fiber-FISH Analysis. *J. Hum. Genet.* **2011**, *56*, 810–812.

11. Marie, R.; Pedersen, J. N.; Bauer, D. L. V.; Rasmussen, K. H.; Yusuf, M.; Volpi, E.; Flyvbjerg, H.; Kristensen, A.; Mir, K. U. Integrated View of Genome Structure and Sequence of a Single DNA Molecule in a Nanofluidic Device. *Proc. Natl. Acad. Sci. U.S.A.* **2013**, *110*, 4893–4898.

12. Hastie, A. R.; Dong, L.; Smith, A.; Finklestein, J.; Lam, E. T.; Huo, N.; Cao, H.; Kwok, P.-Y.; Deal, K. R.; Dvorak, J.; et al. Rapid Genome Mapping in Nanochannel Arrays for Highly Complete and Accurate De Novo Sequence Assembly of the Complex Aegilops tauschii Genome. *PLoS One* **2013**, *8*, e55864.

13. Lam, E. T.; Hastie, A.; Lin, C.; Ehrlich, D.; Das, S. K.; Austin, M. D.; Deshpande, P.; Cao, H.; Nagarajan, N.; Xiao, M.; et al. Genome Mapping on Nanochannel Arrays for Structural Variation Analysis and Sequence Assembly. *Nat. Biotechnol.* **2012**, *30*, 771–776.

14. Reisner, W.; Larsen, N. B.; Silahtaroglu, A.; Kristensen, A.; Tommerup, N.; Tegenfeldt, J. O.; Flyvbjerg, H. Single-Molecule Denaturation Mapping of DNA in Nanofluidic Channels. *Proc. Natl. Acad. Sci. U.S.A.* **2010**, *107*, 13294–13299.

15. Baday, M.; Cravens, A.; Hastie, A.; Kim, H.; Kudeki, D. E.; Kwok, P.-Y.; Xiao, M.; Selvin, P. R. Multicolor Super-Resolution DNA Imaging for Genetic Analysis. *Nano Lett.* **2012**, *12*, 3861–3866.

16. Cheeseman, K.; Rouleau, E.; Vannier, A.; Thomas, A.; Briaux, A.; Lefol, C.; Walrafen, P.; Bensimon, A.; Lidereau, R.; Conseiller, E.; et al. A Diagnostic Genetic Test for the Physical Mapping of Germline Rearrangements in the Susceptibility Breast Cancer Genes BRCA1 and BRCA2. *Hum. Mutat.* **2012**, *33*, 998–1009.

17. Gad, S.; Klinger, M.; Caux-Moncoutier, V.; Pages-Berhouet, S.; Gauthier-Villars, M.; Coupier, I.; Bensimon, A.; Aurias, A.; Stoppa-Lyonnet, D. Bar Code Screening on Combed DNA for Large Rearrangements of the BRCA1 and BRCA2 Genes in French Breast Cancer Families. *J. Med. Genet.* **2002**, *39*, 817–821.

18. Mahiet, C.; Ergani, A.; Huot, N.; Alende, N.; Azough, A.; Salvaire, F.; Bensimon, A.; Conseiller, E.; Wain-Hobson, S.; Labetoulle, M.; et al. Structural Variability of the Herpes Simplex Virus 1 Genome *In Vitro* and *In Vivo*. *J. Virol.* **2012**, *86*, 8592–8601.

19. Nguyen, K.; Walrafen, P.; Bernard, R.; Attarian, S.; Chaix, C.; Vovan, C.; Renard, E.; Dufrane, N.; Pouget, J.; Vannier, A.; et al. Molecular Combing Reveals Allelic Combinations in

Facioscapulohumeral Dystrophy. *Ann. Neurol.* **2011**, *70*, 627–633.

20. Levy-Sakin, M.; Grunwald, A.; Kim, S.; Gassman, N. R.; Gottfried, A.; Antelman, J.; Kim, Y.; Ho, S. O.; Samuel, R.; Michalet, X.; et al. Toward Single-Molecule Optical Mapping of the Epigenome. *ACS Nano* **2013**, *8*, 14–26.

21. Wang, K.; Zhang, W.; Jiang, Y.; Zhang, T. Systematic Application of DNA Fiber-FISH Technique in Cotton. *PLoS One* **2013**, *8*, e75674.

22. Koo, D. H.; Han, F.; Birchler, J. A.; Jiang, J. Distinct DNA Methylation Patterns Associated with Active and Inactive Centromeres of the Maize B Chromosome. *Genome Res.* **2011**, *21*, 908–914.

23. Ananiev, G. E.; Goldstein, S.; Runnheim, R.; Forrest, D. K.; Zhou, S.; Potamousis, K.; Churas, C. P.; Bergendahl, V.; Thomson, J. A.; Schwartz, D. C. Optical Mapping Discerns Genome Wide DNA Methylation Profiles. *BMC Mol. Biol.* **2008**, *9*, 68.

24. Bell, D. C.; Thomas, W. K.; Murtagh, K. M.; Dionne, C. A.; Graham, A. C.; Anderson, J. E.; Glover, W. R. DNA Base Identification by Electron Microscopy. *Microsc. Microanal.* **2012**, *18*, 1049–1053.

25. Wang, X.; Takebayashi, S.-i.; Bernardin, E.; Gilbert, D.; Chella, R.; Guan, J. Microfluidic Extraction and Stretching of Chromosomal DNA from Single Cell Nuclei for DNA Fluorescence In-Situ Hybridization. *Biomed. Microdevices* **2012**, *14*, 443–451.

26. Bensimon, D.; Simon, A. J.; Croquette, V.; Bensimon, A. Stretching DNA with a Receding Meniscus: Experiments and Models. *Phys. Rev. Lett.* **1995**, *74*, 4754–4757.

27. Meng, X.; Benson, K.; Chada, K.; Huff, E. J.; Schwartz, D. C. Optical Mapping of Lambda Bacteriophage Clones Using Restriction Endonucleases. *Nat. Genet.* **1995**, *9*, 432–438.

28. Perkins, T. T.; Smith, D. E.; Chu, S. Single Polymer Dynamics in an Elongational Flow. *Science* **1997**, *276*, 2016–2021.

29. Dimalanta, E. T.; Lim, A.; Runnheim, R.; Lamers, C.; Churas, C.; Forrest, D. K.; de Pablo, J. J.; Graham, M. D.; Coppersmith, S. N.; Goldstein, S.; et al. A Microfluidic System for Large DNA Molecule Arrays. *Anal. Chem.* **2004**, *76*, 5293–5301.

30. Yokota, H.; Sunwoo, J.; Sarikaya, M.; van den Engh, G.; Aebersold, R. Spin-Stretching of DNA and Protein Molecules for Detection by Fluorescence and Atomic Force Microscopy. *Anal. Chem.* **1999**, *71*, 4418–4422.

31. Kim, J. H.; Shi, W.-X.; Larson, R. G. Methods of Stretching DNA Molecules Using Flow Fields. *Langmuir* **2006**, *23*, 755–764.

32. Jing, J.; Reed, J.; Huang, J.; Hu, X.; Clarke, V.; Edington, J.; Housman, D.; Anantharaman, T. S.; Huff, E. J.; Mishra, B.; et al. Automated High Resolution Optical Mapping Using Arrayed, Fluid-Fixed DNA Molecules. *Proc. Natl. Acad. Sci. U.S.A.* **1998**, *95*, 8046–8051.

33. Wang, W.; Lin, J.; Schwartz, D. C. Scanning Force Microscopy of DNA Molecules Elongated by Convective Fluid Flow in an Evaporating Droplet. *Biophys. J.* **1998**, *75*, 513–520.

34. Chan, T.-F.; Ha, C.; Phong, A.; Cai, D.; Wan, E.; Leung, L.; Kwok, P.-Y.; Xiao, M. A Simple DNA Stretching Method for Fluorescence Imaging of Single DNA Molecules. *Nucleic Acids Res.* **2006**, *34*, e113.

35. Lim, A.; Dimalanta, E. T.; Potamousis, K. D.; Yen, G.; Apodoca, J.; Tao, C.; Lin, J.; Qi, R.; Skiadas, J.; Ramanathan, A.; et al. Shotgun Optical Maps of the Whole Escherichia coli O157:H7 Genome. *Genome Res.* **2001**, *11*, 1584–1593.

36. Allemand, J. F.; Bensimon, D.; Jullien, L.; Bensimon, A.; Croquette, V. pH-Dependent Specific Binding and Combing of DNA. *Biophys. J.* **1997**, *73*, 2064–2070.

37. Bensimon, A.; Simon, A.; Chiffaudel, A.; Croquette, V.; Heslot, F.; Bensimon, D. Alignment and Sensitive Detection of DNA by a Moving Interface. *Science* **1994**, *265*, 2096–2098.

38. Kudo, H.; Suga, K.; Fujihira, M. Fabrication of Substrates with Various Wettabilities for DNA Molecular Combing. *Colloids Surf., A* **2008**, *313–314*, 651–654.

39. Liu, Y.-Y.; Wang, P.-Y.; Dou, S.-X.; Wang, W.-C.; Xie, P.; Yin, H.-W.; Zhang, X.-D.; Xi, X. G. Ionic Effect on Combing of Single DNA Molecules and Observation of their Force-Induced Melting by Fluorescence Microscopy. *J. Chem. Phys.* **2004**, *121*, 4302–4309.

40. Benke, A.; Mertig, M.; Pompe, W. pH- and Salt-Dependent Molecular Combing of DNA: Experiments and Phenomenological Model. *Nanotechnology* **2011**, *22*, 035304.

41. Gueroui, Z.; Place, C.; Freyssingeas, E.; Berge, B. Observation by Fluorescence Microscopy of Transcription on Single Combed DNA. *Proc. Natl. Acad. Sci. U.S.A.* **2002**, *99*, 6005–6010.

42. Kwak, K. J.; Kudo, H.; Fujihira, M. Imaging Stretched Single DNA Molecules by Pulsed-Force-Mode Atomic Force Microscopy. *Ultramicroscopy* **2003**, *97*, 249–255.

43. Deegan, R. D.; Bakajin, O.; Dupont, T. F.; Huber, G.; Nagel, S. R.; Witten, T. A. Capillary Flow as the Cause of Ring Stains from Dried Liquid Drops. *Nature* **1997**, *389*, 827–829.

44. Sugimura, H.; Hozumi, A.; Kameyama, T.; Takai, O. Organosilane Self-Assembled Monolayers Formed at the Vapour/Solid Interface. *Surf. Interface Anal.* **2002**, *34*, 550–554.

45. Fiorilli, S.; Rivolo, P.; Descrovi, E.; Ricciardi, C.; Pasquardini, L.; Lunelli, L.; Vanzetti, L.; Pederzolli, C.; Onida, B.; Garrone, E. Vapor-Phase Self-Assembled Monolayers of Aminosilane on Plasma-Activated Silicon Substrates. *Colloids Surf., A* **2008**, *321*, 235–241.

46. Ito, Y.; Virkar, A. A.; Mannsfeld, S.; Oh, J. H.; Toney, M.; Locklin, J.; Bao, Z. Crystalline Ultrasmooth Self-Assembled Monolayers of Alkylsilanes for Organic Field-Effect Transistors. *J. Am. Chem. Soc.* **2009**, *131*, 9396–9404.

47. Wang, Y.; Lieberman, M. Growth of Ultrasmooth Octadecyltrichlorosilane Self-Assembled Monolayers on SiO_2. *Langmuir* **2003**, *19*, 1159–1167.

48. Picknett, R. G.; Bexon, R. The evaporation of sessile or pendant drops in still air. *J. Colloid Interface Sci.* **1977**, *61*, 336–350.

49. Mognetti, B. M.; Kusumaatmaja, H.; Yeomans, J. M. Drop Dynamics on Hydrophobic and Superhydrophobic Surfaces. *Faraday Discuss.* **2010**, *146*, 153–165.

50. Thampi, S. P.; Adhikari, R.; Govindarajan, R. Do Liquid Drops Roll or Slide on Inclined Surfaces? *Langmuir* **2013**, *29*, 3339–3346.

51. Vranken, C.; Deen, J.; Dirix, L.; Stakenborg, T.; Dehaen, W.; Leen, V.; Hofkens, J.; Neely, R. K. Super-resolution optical DNA Mapping *via* DNA methyltransferase-directed click chemistry. *Nucleic Acids Res.* **2014**, *42*, e50.

52. Voet, T.; Macaulay, I. C. Single cell genomics: advances and future perspectives. *PLoS Genet.* **2014**, *10*, e1004126.